Inorganic Chemistry
Article

Inorg. Chem. **2010**, *49*, 4117–4124 **4117**
DOI: 10.1021/ic902178c

Self-Assembly of Metal−Organic Supramolecules: From a Metallamacrocycle and a Metal−Organic Coordination Cage to 1D or 2D Coordination Polymers Based on Flexible Dicarboxylate Ligands

Fangna Dai,[†] Jianmin Dou,[‡] Haiyan He,[†] Xiaoliang Zhao,[†] and Daofeng Sun*[,†]

[†]*Key Lab of Colloid and Interface Chemistry, Ministry of Education, School of Chemistry and Chemical Engineering, Shandong University, Jinan 250100, People's Republic of China, and* [‡]*Department of Chemistry, Liaocheng University, Liaocheng 252059, People's Republic of China*

Received November 4, 2009

To assemble metal−organic supramolecules such as a metallamacrcocycle and metal−organic coordination cage (MOCC), a series of flexible dicarboxylate ligands with the appropriate angle, 2,2′-(2,3,5,6-tetramethyl-1,4-phenylene)-bis(methylene)bis(sulfanediyl)dibenzoic acid ($H_2\mathbf{L}^1$), 2,2′-(2,5-dimethyl-1,4-phenylene)bis(methylene)bis(sulfanediyl)-dibenzoic acid ($H_2\mathbf{L}^2$), 2,2′-(2,4,6-trimethyl-1,3-phenylene)bis(methylene)bis(sulfanediyl)dinicotinic acid ($H_2\mathbf{L}^3$), and 2,2′-(2,4,6-trimethyl-1,3-phenylene)bis(methylene)bis(sulfanediyl)dibenzoic acid ($H_2\mathbf{L}^4$), have been designed and synthesized. Using these flexible ligands to assemble with metal ions, six metal−organic supramolecules, $Cd_2(\mathbf{L}^1)_2(dmf)_4(H_2O)_2\cdot H_2O$ (**1**), $Mn_3(^1\mathbf{L}^2)_2(^2\mathbf{L}^2)(dmf)_2(H_2O)_2\cdot 5dmf$ (**2**), $Cu_4(\mathbf{L}^3)_4(H_2O)_4\cdot 3dmf$ (**3**), $Cu_4(\mathbf{L}^4)_4(dmf)_2(EtOH)_2\cdot 8dmf\cdot 6H_2O$ (**4**), $Mn_4(\mathbf{L}^4)_4(dmf)_4(H_2O)_4\cdot 6dmf\cdot H_2O$ (**5**), and $Mn_3(\mathbf{L}^4)_3(dmf)_4\cdot 2dmf\cdot 3H_2O$ (**6**), possessing a rectangular macrocycle, MOCCs or their extensions, and 1D or 2D coordination polymers, have been isolated. All complexes have been characterized by single-crystal X-ray diffraction, elemental analysis, and thermogravimetric analysis. Complex **1** is a discrete rectangular macrocycle, while complex **2** is a 2D macrocycle-based coordination polymer in which the $\mathbf{L}^2$ ligand adopts both syn and anti conformations. Complexes **3**−**5** are discrete MOCCs in which two binuclear metal clusters are engaged by four organic ligands. The different geometries of the secondary building units (SBUs) and the axial coordinated solvates on the SBUs result in their different symmetries. Complex **6** is a 1D coordination polymer, extended from a MOCC made up of two metal ions and three $\mathbf{L}^4$ ligands. All of the flexible dicarboxylate ligands adopt a syn conformation except that in complex **2**, indicating that the syn conformational ligand is helpful for the formation of a metallamacrocycle and a MOCC. The magnetic properties of complexes **5** and **6** have also been studied.

Introduction

Self-organization or self-assembly is an essential process in supramolecular chemistry and biology.[1] Recently, with the development of supramolecular chemistry and engineering, self-assembly by engaging an organic ligand and metal ion or cluster through coordinative bond or supramolecular interactions such as hydrogen bonds, $\pi\cdots\pi$ interactions, etc., to generate desired topological structures has become an important process in the construction of metal−organic supramolecules such as discrete metal−organic coordination cages (MOCCs), nanoballs, metallamacrocycles, and multidimensional open frameworks.[2,3]

As is known, the self-assembly of discrete supramolecules is highly determined by the ligand geometry and the coordination geometry of the metal ions. Thus, selecting a suitable organic ligand with certain features, such as flexibility, appropriate angles, and versatile binding modes, to coordinate to the metal ion with plastic coordination geometry is crucial to the construction of discrete supramolecules. In the past decades, many discrete metallamacrocycles and MOCCs or polygons have been designed and synthesized. In particular, Stang and Olenyuk reported a series of metallamacrocycles

*To whom correspondence should be addressed. E-mail: dfsun@sdu.edu.cn.

(1) Lehn, J.-M. *Angew. Chem., Int. Ed.* **1988**, *27*, 89.

(2) (a) Batten, S. R.; Robson, R. *Angew. Chem., Int. Ed.* **1998**, *37*, 1460. (b) Leininger, S.; Olenyuk, B.; Stang, P. J. *Chem. Rev.* **2000**, *100*, 853. (c) Keefe, M. H.; Benkstein, K. D.; Hupp, J. T. *Coord. Chem. Rev.* **2000**, *205*, 201. (d) Eddaoudi, M.; Moler, D. B.; Chen, B.; Reineke, T. M.; O'Keeffe, M.; Yaghi, O. M. *Acc. Chem. Rev.* **2001**, *34*, 319. (e) Fijita, M.; Ogura, K. *Coord. Chem. Rev.* **1996**, *148*, 249.

(3) (a) Kitagawa, S.; Kitaura, R.; Noro, S.-I. *Angew. Chem., Int. Ed.* **2004**, *43*, 2334. (b) Seo, J. S.; Whang, D.; Lee, H.; Jun, S. I.; Oh, J.; Young, J.; Kim, K. *Nature* **2000**, *404*, 982. (c) Fiedler, D.; Leung, D. H.; Bergman, R. G.; Raymond, K. N. *Acc. Chem. Rev.* **2005**, *38*, 349. (d) MacGillivray, L. R.; Atwood, J. L. *J. Solid State Chem.* **2000**, *152*, 199.

Published on Web 04/09/2010

based on palladium, platinum, and rigid pyridine-containing ligands.[4] Yaghi et al.[5] and Zaworotko et al.[6] reported the design and synthesis of discrete cages or polygons by using 120° angular dicarboxylate ligands. Raymond et al. synthesized a series of polyhedral structures based on bis(catecholate) ligands and tested their catalysis properties.[7] The MOCCs constructed from N-containing ligands have also been independently reported by Fujita and Hong groups.[8]

Most of the organic ligands in the reported work as mentioned above are limited to a rigid angular carboxylate and an N-containing ligand as well as a bis(catecholate) ligand with the appropriate chelating ability. However, the role of a flexible carboxylate ligand with the appropriate angle in the construction of metallamacrocycles and MOCC is somewhat ignored. Indeed, compared to rigid organic ligands, flexible ones can change their conformations to meet the coordination requirement of the metal ion, which can result in more topological structures than the rigid ligand.[9] For example, Sun and co-workers have synthesized a series of metal−organic frameworks based on flexible tripodal ligands such as benzene-1,3,5-triacetate, 1,3,5-tris(imidazol-1-ylmethyl)-2,4,6-trimethylbenzene, and their derivatives,[10,11] in which the flexible tripodal ligands can adopt cis,trans,trans or cis,cis,cis conformation based on the requirement of the metal ions or the 3D packing. Thus, it is possible to construct discrete molecules such as metallamacrocycles and MOCCs based on a flexible carboxylate ligand with the appropriate angle by careful design.

With these considerations in mind, recently, we designed a flexible dicarboxylate ligand, 2,2′-(2,4,6-trimethyl-1,3-phenylene)bis(methylene)bis(sulfanediyl)dibenzoic acid (H_2L^4), which can adopt syn and anti conformations based on the location of the two substituted benzoic acid groups. The two benzoic acid groups located in the meta position of the central benzene ring and the linker $-SCH_2-$ between the central benzene ring and benzoic acid provide flexibility of the ligand. By using this new ligand to assemble with manganese ion, a novel MOCC, $Mn_4(\mathbf{L}^4)_4(dmf)_4(H_2O)_4\cdot 6dmf\cdot H_2O$ (**5**), has been synthesized.[12] To extend our previous work, we have endeavored to carry out a systematic study of the construction of metal−organic supramolecules such as metallamacrocycles, MOCCs, and their derivatives based on flexible dicarboxylate ligands by synthesizing a series of flexible dicarboxylate ligands with the appropriate angles to assemble with various metal ions (Scheme 1). In this full paper, we describe the details of the syntheses, characterizations, and properties of six metal−organic supramolecules based on flexible dicarboxylate ligands, $Cd_2(\mathbf{L}^1)_2(dmf)_4(H_2O)_2\cdot H_2O$ (**1**), $Mn_3(^1\mathbf{L}^2)_2(^2\mathbf{L}^2)(dmf)_2(H_2O)_2\cdot 5dmf$ (**2**), $Cu_4(\mathbf{L}^3)_4(H_2O)_4\cdot 3dmf$ (**3**), $Cu_4(\mathbf{L}^4)_4(dmf)_2(EtOH)_2\cdot 8dmf\cdot 6H_2O$ (**4**), $Mn_4(\mathbf{L}^4)_4(dmf)_4(H_2O)_4\cdot 6dmf\cdot H_2O$ (**5**), and $Mn_3(\mathbf{L}^4)_3(dmf)_4\cdot 2dmf\cdot 3H_2O$ (**6**), which possess metallamacrocycles, MOCCs, and 1D or 2D coordination polymers.

Scheme 1. Designed Flexible Dicarboxylate Ligands

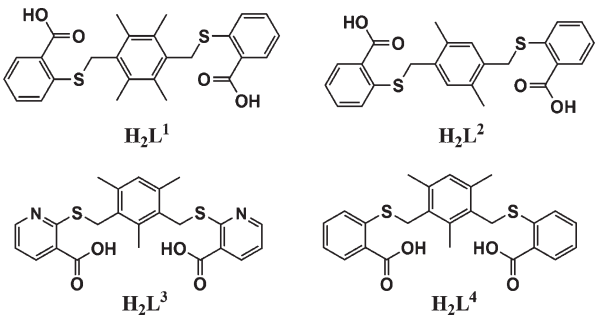

Experimental Section

Materials and Physical Measurements. All of the starting materials used were used as purchased without further purification. C, H, N, and S microanalyses were carried out in the elementary analysis group of this department. Thermogravimetric analysis (TGA) experiments were performed using a TGA/SDTA851 instrument (heating rate of 10 °C min^{-1}; nitrogen stream).

Synthesis of H_2L^1. Sodium methoxide (1.62 g, 30 mmol) was dissolved in absolute methanol (MeOH; 200 mL) and cooled to room temperature. 2-Mercaptobenzoic acid (4.63 g, 30 mmol) was then added with stirring, and stirring was continued for 10 min. To the resulting suspension was added 1,4-bis(bromomethyl)-2,3,5,6-tetramethylbenzene (3.2 g, 10 mmol), and the reaction mixture was stirred under reflux for 6 h. The solid was filtered while still hot, dissolved in water (H_2O), and filtered to remove any undissolved substance. The filtrate was acidified with dilute hydrochloric acid, and the precipitates were filtered and washed with H_2O and hot MeOH. Yield: 45%. ^1H NMR (300 MHz, DMSO-d_6): δ 2.23 (s, 12 H), 4.66 (s, 4 H), 6.98−7.10 (m, 4 H), 7.18−7.23 (m, 4 H).

Synthesis of H_2L^2. H_2L^2 was prepared by a route similar to that of H_2L^1 but using 1,4-bis(bromomethyl)-2,5-dimethylbenzene (2.92 g, 10 mmol) instead. Yield: 50%. ^1H NMR (300 MHz, DMSO-d_6): δ 2.31 (s, 6 H), 4.11 (s, 4 H), 7.91 (s, 2 H), 7.52 (m, 4 H), 7.21 (m, 4 H).

(4) Stang, P. J.; Olenyuk, B. *Acc. Chem. Res.* **1997**, *30*, 502 and references cited therein.

(5) (a) Eddaoudi, M.; Kim, J.; Wachter, J. B.; Chae, H. K.; O'Keeffe, M.; Yaghi, O. M. *J. Am. Chem. Soc.* **2001**, *123*, 4368. (b) Ni, Z.; Yassar, A.; Antoun, T.; Yaghi, O. M. *J. Am. Chem. Soc.* **2005**, *127*, 12752. (c) Furukawa, H.; Kim, J.; Plass, K. E.; Yaghi, O. M. *J. Am. Chem. Soc.* **2006**, *128*, 8398.

(6) (a) Lu, J.; Mondal, A.; Moulton, B.; Zaworotko, M. J. *Angew. Chem., Int. Ed.* **2001**, *40*, 2113. (b) Moulton, B.; Lu, J.; Mondal, A.; Zaworotko, M. J. *Chem. Commun.* **2001**, 863. (c) Boume, S. A.; Lu, J.; Mondal, A.; Moulton, B.; Zaworotko, M. J. *Angew. Chem., Int. Ed.* **2001**, *40*, 2111.

(7) (a) Leung, D. H.; Fiedler, D.; Bergman, R. G.; Raymond, K. N. *Angew. Chem., Int. Ed.* **2004**, *43*, 963. (b) Miranda, J. J.; Andersen, U. N.; Johnson, D. W.; Leary, J. A.; Raymond, K. N. *Angew. Chem., Int. Ed.* **2001**, *40*, 733. (c) Sun, X. K.; Johnson, D. W.; Caulder, D. L.; Powers, R. E.; Raymond, K. N.; Wong, E. H. *Angew. Chem., Int. Ed.* **1999**, *38*, 1303. (d) Caulder, D. L.; Powers, R. E.; Parac, T. N.; Raymond, K. N. *Angew. Chem., Int. Ed.* **1998**, *37*, 1840. (e) Fiedler, D.; Bergman, R. G.; Raymond, K. N. *Angew. Chem., Int. Ed.* **2004**, *43*, 6748.

(8) (a) Yoshizawa, M.; Tamura, M.; Fujita, M. *Science* **2006**, *312*, 251. (b) Fujita, M.; Fujita, N.; Ogura, K.; Yamaguchik, K. *Nature* **1999**, *400*, 52. (c) Hong, M. C.; Zhao, Y. J.; Su, W. P.; Cao, R.; Fujita, M.; Zhou, Z. Y.; Chan, A. S. C. *J. Am. Chem. Soc.* **2000**, *122*, 4819.

(9) Lee, E.; Kim, Y.; Jung, D. Y. *Inorg. Chem.* **2002**, *41*, 501.

(10) (a) Wan, S.-Y.; Li, Y.-Z.; Okamura, T.; Fan, J.; Sun, W.-Y.; Ueyama, N. *Eur. J. Inorg. Chem.* **2003**, 3783. (b) Zhang, Z.-H.; Shen, Z.-L.; Okamura, T.; Zhu, H.-F.; Sun, W.-Y.; Ueyama, N. *Cryst. Growth Des.* **2005**, *5*, 1191. (c) Liu, G.-X.; Huang, Y.-Q.; Chu, Q.; Okamura, T.; Sun, W.-Y.; Liang, H.; Ueyama, N. *Cryst. Growth Des.* **2008**, *8*, 3233. (d) Zhang, Z.-H.; Okamura, T.; Hasegawa, Y.; Kawaguchi, H.; Kong, L.-Y. *Inorg. Chem.* **2005**, *44*, 6219. (e) Zhu, H.-F.; Fan, J.; Okamura, T.; Zhang, Z.-H.; Liu, G.-X.; Yu, K.-B. *Inorg. Chem.* **2006**, *45*, 3941.

(11) (a) Wang, Y.; Huang, Y.-Q.; Liu, G.-X.; Okamura, T.; Doi, M.; Sheng, Y.-W.; Sun, W.-Y.; Ueyama, N. *Chem.—Eur. J.* **2007**, *13*, 7523. (b) Fan, J.; Gan, L.; Kawaguchi, H.; Sun, W.-Y.; Yu, K.-B.; Tang, W.-X. *Chem.—Eur. J.* **2003**, *9*, 3965. (c) Zhao, W.; Song, Y.; Okamura, T.; Fan, J.; Sun, W.-Y.; Ueyama, N. *Inorg. Chem.* **2005**, *44*, 3330. (d) Zhang, Z.-H.; Song, Y.; Okamura, T.; Hasegawa, Y.; Sun, W.-Y.; Ueyama, N. *Inorg. Chem.* **2006**, *45*, 2896. (e) Sun, W.-Y.; Fan, J.; Okamura, T.; Xie, J.; Yu, K.-B.; Ueyama, N. *Chem.—Eur. J.* **2001**, *7*, 2557.

(12) Dai, F. N.; He, H. Y.; Xie, A. P.; Chu, G. D.; Sun, D. F.; Ke, Y. X. *CrystEngComm* **2009**, *11*, 47.

Synthesis of H_2L^3. Sodium (0.6 g, 30 mmol) was added to 200 mL of absolute ethanol (EtOH) in a 500 mL flask, and after the sodium disappeared, the mixture was then cooled to room temperature. 2-Mercaptonicotinic acid (4.66 g, 30 mmol) was then added under nitrogen with stirring, and stirring was continued for 10 min. To the resulting suspension was added 2,4-bis(bromomethyl)-1,3,5-trimethylbenzene (3.06 g, 10 mmol), and the reaction mixture was stirred under reflux for 6 h. The solid was filtered while still hot, dissolved in H_2O, and filtered to remove any undissolved substance. The filtrate was acidified with dilute hydrochloric acid, and the precipitates were filtered and washed with H_2O and hot EtOH. Yield: 60%. ^{1}H NMR (300 MHz, DMSO-d_6): δ 2.31 (s, 3 H), 2.34 (s, 6 H), 4.36 (s, 4 H), 7.31 (s, 1 H), 8.28 (d, 2 H, Ph−H^4), 8.50 (t, 2 H), 8.71 (d, 2 H).

Synthesis of H_2L^4. H_2L^4 was prepared by a route similar to that of H_2L^1 but using 2,4-bis(bromomethyl)-1,3,5-trimethylbenzene (3.06 g, 10 mmol) instead. Yield: 70%. ^{1}H NMR (300 MHz, DMSO-d_6): δ 2.35 (s, 3 H), 2.41 (s, 6 H), 4.15 (s, 4 H), 6.41 (s, 1 H), 6.98 (t, 2 H), 7.26 (d, 2 H), 7.58 (t, 2 H), 7.92 (d, 2 H).

Preparation of Metal−Organic Supramolecules. $Cd_2(L^1)_2(dmf)_4(H_2O)_2\cdot H_2O$ (1). $Cd(NO_3)_2\cdot 4H_2O$ (0.01 g, 0.03 mmol), H_2L^1 (0.01 g, 0.021 mmol), and NEt_3 (1 drop) were dissolved in 16 mL of mixed solvents of *N*,*N*-dimethylformamide (DMF), EtOH, and H_2O (5:2:1, v/v) and heated in a Telfon-lined steel bomb at 80 °C for 3 days. The colorless crystalline block that formed was collected, washed with H_2O, and dried in the air. Yield: 40%. Elem anal. Calcd for **1**: C, 51.23; H, 5.51; N, 3.73; S, 8.55. Found: C, 51.45; H, 5.22; N, 3.59, S, 8.99.

$Mn_3(^1L^2)_2(^2L^2)(dmf)_2(H_2O)_2\cdot 5dmf$ (2). $Mn(OAc)_2\cdot 4H_2O$ (0.02 g, 0.08 mmol), H_2L^2 (0.01 g, 0.023 mmol), and melamine (0.01 g, 0.08 mmol) were dissolved in 10 mL of mixed solvents of DMF, EtOH, and H_2O (5:2:1, v/v) in a 25 mL beaker. After stirring at room temperature for 10 min, the beaker was left at 80 °C for 2 days. The resulting brown block crystals of **2** were collected in 55% yield on the basis of manganese. Elem anal. Calcd for **2**: C, 55.59; H, 5.72; N, 4.19; S, 9.56. Found: C, 55.47 H, 5.68; N, 4.62; S, 9.74.

$Cu_4(L^3)_4(H_2O)_4\cdot 3dmf$ (3). $Cu(NO_3)_2\cdot 3H_2O$ (0.01 g, 0.04 mmol), H_2L^3 (0.01 g, 0.022 mmol), and NEt_3 (1 drop) were dissolved in 10 mL of DMF in a 25 mL beaker. After stirring at room temperature for 10 min, the beaker was left at 100 °C for 3 days. The resulting blue block crystals of **3** were collected in 60% yield on the basis of copper. Elem anal. Calcd for **3**: C, 51.55; H, 4.67; N, 6.55; S, 10.88. Found: C, 51.83; H, 4.71; N, 6.60; S, 10.51.

$Cu_4(L^4)_4(dmf)_2(EtOH)_2\cdot 8dmf\cdot 6H_2O$ (4). $Cu(NO_3)_2\cdot 3H_2O$ (0.01 g, 0.04 mmol), H_2L^4 (0.01 g, 0.022 mmol), and NEt_3 (1 drop) were dissolved in 10 mL of mixed solvents of DMF, EtOH, and H_2O (5:2:1, v/v) in a 25 mL beaker. After stirring at room temperature for 10 min, the beaker was left at 60 °C for 6 days. The resulting blue block crystals of **4** were collected in 75% yield on the basis of copper. Elem anal. Calcd for **4**: C, 53.87; H, 6.14; N, 4.69; S, 8.58. Found: C, 53.17; H, 6.06; N, 4.46, S 8.37.

$Mn_4(L^4)_4(dmf)_4(H_2O)_4\cdot 6dmf\cdot H_2O$ (5). $Mn(OAc)_2\cdot 4H_2O$ (0.02 g, 0.08 mmol) and H_2L^4 (0.02 g, 0.044 mmol) were dissolved in a 16 mL mixture of DMF, EtOH, and H_2O (5:2:1, v/v), to which 2 drops of pyridine was added with stirring. The solution was filtered, and the filtrate was allowed to evaporate at room temperature for 2 days to give rise to a large amount of colorless block crystals of **5**. Yield: 55%. Elem anal. Calcd for **5**: C, 54.92; H, 5.96; N, 4.93; S, 9.02. Found: C, 54.18; H, 6.04; N, 4.91; S, 9.31.

$Mn_3(L^4)_3(dmf)_4\cdot 2dmf\cdot 3H_2O$ (6). H_2L^4 (0.02 g, 0.044 mmol) and $Mn(OAc)_2\cdot 4H_2O$ (0.02 g, 0.08 mmol) were dissolved in 16 mL of DMF. The mixture was heated in a Teflon-coated steel autoclave at 80 °C for 66 h and then cooled at a rate of ca. 5 °C m^{-1} to room temperature to give light-brown crystals of **6**. Yield: 52%. Elem anal. Calcd for **6**: C, 55.60; H, 5.72; N, 4.18; S, 9.57. Found: C, 55.47; H, 5.68; N, 4.62; S, 9.74.

X-ray Structural Crystallography. Crystals of **1**−**6** mounted on a glass fiber were studied with a Bruker APEXII CCD single-crystal X-ray diffractometer with a graphite-monochromated Mo KR radiation (λ = 0.710 73 Å) source at 25 °C. Absorption corrections were applied using the multiscan program *SADABS*. All structures were solved by direct methods using the *SHELXS* program of the *SHELXTL* package and refined by the full-matrix least-squares method with *SHELXL*. The metal atoms in each complex were located from the *E* maps, and other non-hydrogen atoms were located in successive difference Fourier syntheses and refined with anisotropic thermal parameters on F^2. The organic hydrogen atoms were generated geometrically (C−H = 0.96 Å). The free solvent molecules in complexes **2**, **5**, and **6** are highly disordered, and attempts to locate and refine them were unsuccessful. The *SQUEEZE* program was used to remove scattering from the highly disordered solvent molecules, and a new .HKL file was generated. The structure was solved by using the new generated .HKL file. Crystal data as well as details of the data collection and refinements for **1**−**6** are summarized in Table 1. Crystallographic data (excluding structure factors) for the structures reported in this paper have been deposited in the Cambridge Crystallographic Data Center with CCDC nos. 714743−714746 for complexes **1**−**4**, respectively, 702070 for **5**, and 714747 for **6**.

Results and Discussion

Strategy. As is known, the conformation of the organic ligand and the coordination geometry of the metal ion or cluster are two determining factors and should always be carefully taken into consideration in the design and synthesis of discrete molecules such as metallamacrocycles and MOCCs. Our strategy in the design and synthesis of discrete molecules is to use flexible dicarboxylate ligands with the appropriate angles and conformation to coordinate to metal ions or clusters with certain coordination geometries, providing desired structures (Scheme 2). For example, dicopper paddlewheel secondary building units (SBUs) with planar geometry have been widely used in the construction of porous metal−organic frameworks with high hydrogen storage uptake.[13] If two such planar SBUs are connected by four "staple-like" ligands, a MOCC will be generated. On the other hand, the MOCC with a rigid cluster as the node is quite rare in the literature; however, application of the cluster as a node in the construction of MOCCs can add more active sites of the cage, which is helpful in catalysis and gas storage.

Description of the Crystal Structures. Complexes 1 and 2: a Metallamacrocycle (1) and a 2D Metallamacrocycle-Based Layer (2). Single-crystal X-ray diffraction reveals that complex **1** is a rectangular macrocycle made up of two L^1 ligands and two cadmium ions. The asymmetric unit of **1** consists of one cadmium ion, one L^1 ligand, two coordinated dmf molecules, and one coordinated water molecule. The central cadmium ion is seven-coordinated by four oxygen atoms from two L^1 ligands,

(13) (a) Pan, L.; Sander, M. B.; Huang, X.; Li, J.; Smith, M.; Bittner, E. W.; Bockrath, B. C.; Johnson, J. K. *J. Am. Chem. Soc.* **2004**, *126*, 1308. (b) Nouar, F.; Eubank, J. F.; Bousquet, T.; Wojtas, L.; Zaworotko, M.; Eddaoudi, J. M. *J. Am. Chem. Soc.* **2008**, *130*, 3768. (c) Chen, B. L.; Ockwig, N. W.; Millward, A. R.; Contreras, D. S.; Yaghi, O. M. *Angew. Chem., Int. Ed.* **2005**, *44*, 4745. (d) Lin, X.; Jia, J. H.; Zhao, X. B.; Thomas, K. M.; Blake, A. J.; Walker, G. S.; Champness, N. R.; Hubberstey, P.; Schroder, M. *Angew. Chem., Int. Ed.* **2006**, *45*, 7358. (e) Sun, D. F.; Ma, S. Q.; Ke, Y. X.; Collins, D. J.; Zhou, H.-C. *J. Am. Chem. Soc.* **2006**, *128*, 3896.

Table 1. Crystal Data Collection and Structure Refinement for **1**–**6**

	1	2	3
formula	$C_{64}H_{80}Cd_2N_4O_{14}S_4$	$C_{78}H_{88}Mn_3N_2O_{21}S_6$	$C_{92}H_{136}Cu_4N_8O_{24}S_8$
fw	1482.36	1746.68	2248.73
temp (K)	298(2)	298(2)	298(2)
cryst syst	triclinic	triclinic	tetragonal
space group	$P\bar{1}$	$P\bar{1}$	$I4/m$
a (Å)	8.6117(6)	12.1287(6)	14.9706(2)
b (Å)	12.9678(10)	14.4477(7)	14.9706(2)
c (Å)	16.5318(13)	15.5639(8)	26.6564(9)
α (deg)	100.6370(10)	73.240(4)	90
β (deg)	102.5390(10)	69.2450(10)	90
γ (deg)	105.6650(10)	83.595(4)	90
V (Å^3)	1676.1(2)	2477.0(2)	5974.2(2)
Z	1	1	2
ρ_{calcd} (g cm^3)	1.469	1.171	1.250
μ (mm^{-1})	0.824	0.562	0.906
R1 [$I > 2\sigma(I)$][a]	0.0597	0.0700	0.0625
wR2[b]	0.1630	0.1949	0.1877

	4	5	6
formula	$C_{116}H_{128}Cu_4N_4O_{22}S_8$	$C_{124}H_{152}Mn_4N_8O_{28}S_8$	$C_{87}H_{91}Mn_3N_4O_{16}S_6$
fw	2440.86	2678.78	1805.82
temp (K)	298(2)	298(2)	298(2)
cryst syst	monoclinic	monoclinic	monoclinic
space group	$P2_1/n$	$P21/c$	$P2_1/n$
a (Å)	14.9432(10)	23.922(2)	12.3892(14)
b (Å)	25.1208(16)	23.154(2)	27.469(3)
c (Å)	15.3915(10)	28.130(3)	30.401(3)
α (deg)	90	90	90
β (deg)	91.7360(10)	100.444(2)	91.307(7)
γ (deg)	90	90	90
V (Å^3)	5775.1(7)	15323(3)	10343.1(18)
Z	2	4	1
ρ_{calcd} (g cm^3)	1.404	1.161	1.160
μ (mm^{-1})	0.941	0.494	0.538
R1 [$I > 2\sigma(I)$][a]	0.0463	0.0701	0.0840
wR2[b]	0.1349	0.1866	0.2071

[a] $R1 = \sum||F_o| - |F_c||/\sum|F_o|$. [b] $wR2 = [\sum w(F_o^2 - F_c^2)^2/\sum w(F_o^2)^2]^{1/2}$.

Scheme 2. Strategy for the Design and Synthesis of Discrete Molecules

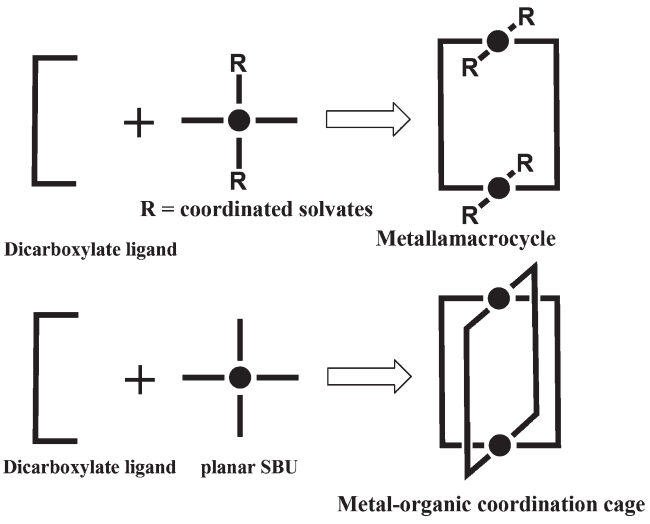

three oxygen atoms from two coordinated dmf molecules, and one coordinated water molecule with an average Cd–O distance of 2.565 Å. Both carboxylate groups of the $\mathbf{L}^1$ ligand adopt a chelating mode to connect one

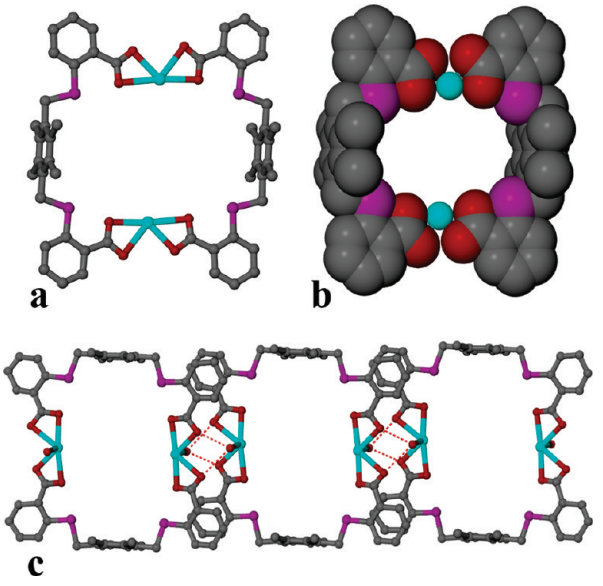

Figure 1. (a and b) Rectangular macrocycle of **1**. (c) 1D supramolecular ladder formed by hydrogen bonding and $\pi\cdots\pi$ interactions between molecules.

cadmium ion. The average dihedral angle between the side benzene ring and the central benzene ring is 87.7°.

Thus, two cadmium ions are connected by two $\mathbf{L}^1$ ligands to generate a rectangular macrocycle with dimensions of 13.3 × 8.6 Å (Figure 1a,b). The remaining coordination sites of the cadmium ion are occupied by coordinated solvates to prevent further extension. The coordinated water molecules and carboxylate oxygen atom provide the hydrogen-bonding donors and acceptors, respectively. Indeed, there are multiple supramolecular interactions in complex **1**, which further connect **1** into a 2D supramolecular architecture. The intermolecular hydrogen-bonding interactions (2.679 and 2.896 Å) between the coordinated water molecule and the two coordinated carboxyl oxygen atoms and the $\pi\cdots\pi$ interactions (3.675 Å) between the side benzene rings in different rectangular macrocycles link the metallamacrocycle to generate a 1D ladder, as shown in Figure 1c. The $\pi\cdots\pi$ interactions (3.625 Å) between the central benzene rings in different macrocycles further connect the 1D ladders to give rise to a 2D layer (Figure 2).

In complex **1**, the flexible $\mathbf{L}^1$ ligand adopts a syn conformation to coordinate to metal ions, providing the rectangular macrocycle. However, if the flexible ligand adopts an anti conformation or a mixture of syn and anti conformations, what kind of structure will result?

Fortunately, when we used $\mathbf{L}^2$ as the ligand to assemble with the manganese ion, complex **2** containing both syn and anti conformations of $\mathbf{L}^2$ was isolated in good yield. Single-crystal X-ray diffraction reveals that complex **2** is a 2D layer framework based on a trinuclear hourglass SBU. The asymmetric unit consists of one and a half manganese ions, one and a half $\mathbf{L}^2$ ligands, one coordinated dmf molecule, one coordinated water molecule, and three uncoordinated water molecules. Both manganese ions are six-coordinated by six oxygen atoms from different $\mathbf{L}^2$ ligands for the Mn1 ion and by four oxygen atoms from different $\mathbf{L}^2$ ligands, one coordinated dmf molecule, and one coordinated water molecule for the Mn2 ion,

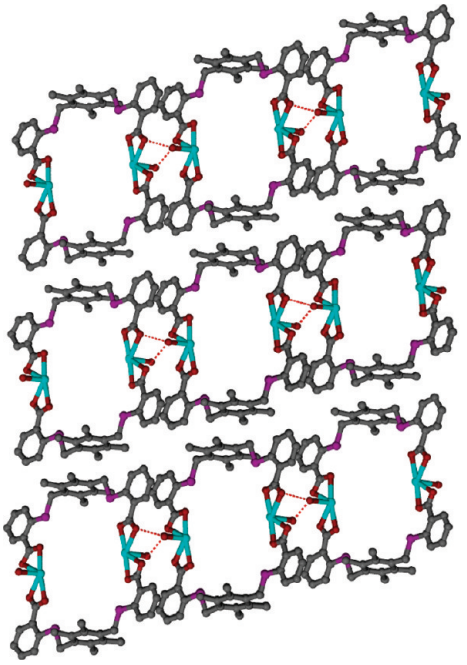

Figure 2. 2D supramolecular layer of **1**.

with average Mn−O distances of 2.169(5) and 2.193(7) Å for Mn1 and Mn2, respectively. One Mn1 and two Mn2 ions are engaged by six carboxylate groups to form a trinuclear hourglass SBU with a Mn1−Mn2 distance of 3.573 Å (Figure 3a), which is similar to other hourglass SBUs found in the reported complexes.[14] There are two types of $\mathbf{L}^2$ ligands, $^1\mathbf{L}^2$ and $^2\mathbf{L}^2$, with different conformations in complex **2**. $^1\mathbf{L}^2$ adopts a syn conformation, with both carboxylate groups located on the same side of the central benzene ring. One carboxylate group of $^1\mathbf{L}^2$ adopts a bidentate bridging mode to bridge two manganese ions, and the other one adopts a chelate bridging mode to chelate and bridge two manganese ions. $^2\mathbf{L}^2$ adopts an anti conformation, with two carboxylate groups located on two sides of the central benzene ring, and both carboxylate groups of $^2\mathbf{L}^2$ adopt a bidentate bridging mode to bridge two manganese ions. The average dihedral angles between the central benzene ring and the side benzene ring are 88° and 91.2° for $^1\mathbf{L}^2$ and $^2\mathbf{L}^2$, respectively.

Thus, the trinuclear "hourglass" SBUs are connected by the $^1\mathbf{L}^2$ ligands along the *b* axis to generate a 1D ladder containing a rectangular macrocycle with dimensions of 12.7 × 8.3 Å (Figure 3b,c), similar to that found in complex **1**. In the 1D ladder (Figure 3d), the $^1\mathbf{L}^2$ ligands act as side pieces and the trinuclear SBUs act as rungs. The 1D ladder is quite similar to the 1D supramolecular ladder formed by $\pi\cdots\pi$ interactions in complex **1** (Figure 1c). There are strong $\pi\cdots\pi$ interactions (3.531 Å) between the side benzene rings in the side pieces of the ladder, which further stabilize the 1D ladder unit. The 1D ladders are further connected by the $^2\mathbf{L}^2$ ligands from above and below the ladders, providing a 2D layer framework with a distance

(14) (a) Chen, W.; Wang, J. Y.; Chen, C.; Yu, Q.; Yuan, H. M.; Chen, J. S.; Wang, S. N. *Inorg. Chem.* **2003**, *4*, 944. (b) Clegg, W.; Little, I. R.; Straughan, B. P. *Inorg. Chem.* **1988**, *27*, 1916. (c) Sun, D. F.; Ke, Y. X.; Collins, D. J.; Lorigan, G. A.; Zhou, H.-C. *Inorg. Chem.* **2007**, *46*, 2725.

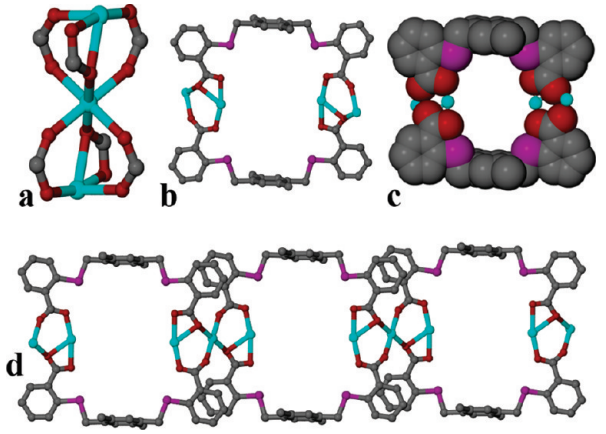

Figure 3. (a) Hourglass SBU in **2**. (b and c) Rectangular macrocycle. (d) 1D ladder formed by $^1\mathbf{L}^2$ ligands.

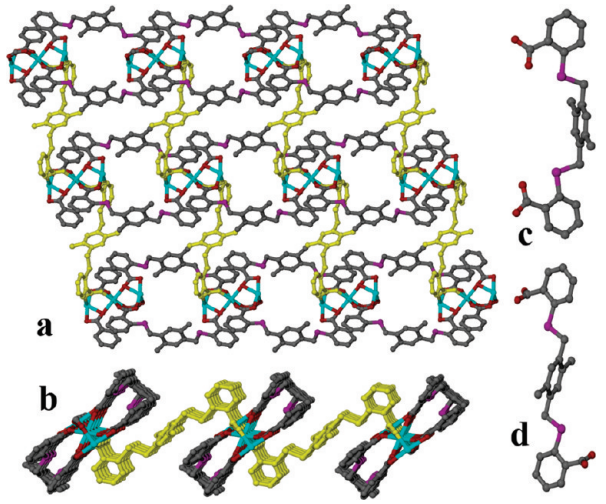

Figure 4. (a and b) 2D layer framework of **2**, with the $^2\mathbf{L}^2$ ligands shown in yellow. (c and d) $^1\mathbf{L}^2$ and $^2\mathbf{L}^2$ ligands in syn and anti conformations, respectively.

between the ladders of 13.49 Å (Figure 4a,b). The strong $\pi\cdots\pi$ interactions (3.511 Å) between the central benzene rings of the $^2\mathbf{L}^2$ ligands in different layers further connect **2** into a 3D supramolecular architecture (Supporting Information).

Complexes 3−6: MOCCs (3−5) and a 1D Cage-Based Coordination Polymer (6). Complexes **3**−**5** are discrete MOCCs based on binuclear SBUs. In these three cagelike complexes, all of the flexible carboxylate ligands adopt a syn conformation to bridge metal ions. The vertexes of the cage are made up of rigid binuclear SBUs, which are rare in the reported cagelike complexes. Although all three MOCCs are made up of four organic ligands and two binuclear SBUs, the different geometries of the SBUs as well as the different coordinated solvates on the axial positions of the SBU make the three MOCCs possess different symmetry.

Complexes **3** and **4** are constructed from well-known dicopper paddlewheel SBUs. Two dicopper SBUs are connected by four $\mathbf{L}^3$ or $\mathbf{L}^4$ ligands for **3** and **4**, respectively, to generate discrete cages. However, the different axially coordinated solvents on the paddlewheel SBUs result in complexes **3** and **4** possessing different symmetries. Single-crystal X-ray diffraction reveals that complex **3** crystallizes

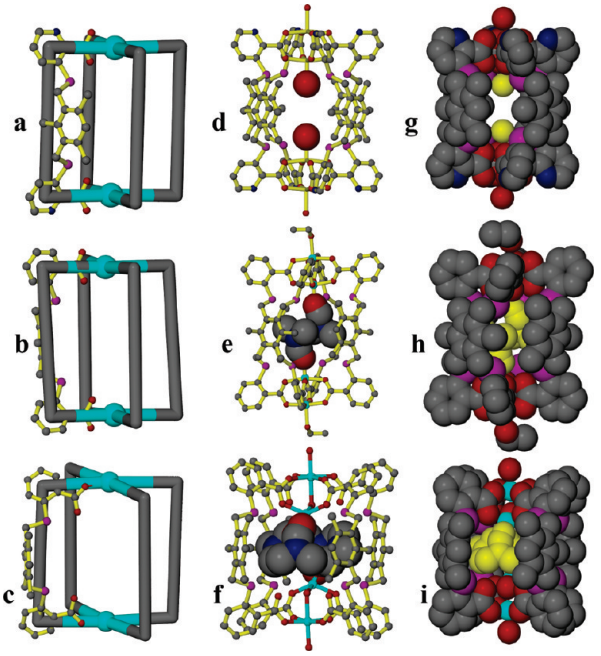

Figure 5. (a−c) Schematic representation of the cages (**3**−**5**, respectively) showing the structure of one of the four identical ligands that span the edges of the cage. (d−f) Crystal structures of the cages (**3**−**5**, respectively) with coordinated solvents inside. (g−i) Space-filling representation of the cages (**3**−**5**, respectively) with coordinated solvents inside of the cages in yellow.

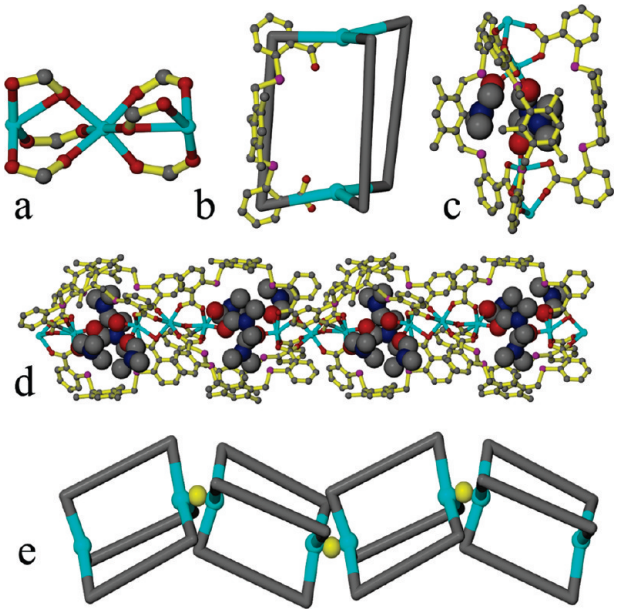

Figure 6. (a) Hourglass SBU in **6**. (b) Schematic representation of the cage showing the structure of one of the three identical ligands that span the edges of the cage. (c) Structures of the cage with coordinated dmf molecules inside. (d) 1D cage-based coordination polymer with coordinated dmf molecules in a space-filling representation inside the cage. (e) Schematic representation showing the 1D cage-based polymer sharing Mn2 ions (yellow ball).

in a tetragonal $I4/m$ space group. The asymmetric unit consists of two demisemi copper ions, half of a $\mathbf{L}^3$ ligand, and two demisemi-coordinated water molecules. Both carboxylate groups of the $\mathbf{L}^3$ ligand adopt a bidentate bridging mode to connect two copper ions. The average dihedral angle between the central benzene ring and the side benzene ring is 117.3°. The axial positions of the paddlewheel SBUs are occupied by two coordinated water molecules. Thus, two paddlewheel SBUs are connected by four $\mathbf{L}^3$ ligands to generate a high symmetry cage with a 4-fold axis passing through the two paddlewheel SBUs (Figure 5a,d,g). The volume of the cage is about 610 $Å^3$. Complex **4** crystallizes in a monoclinic $P2_1/n$ space group. The asymmetric unit consists of two copper ions, two $\mathbf{L}^4$ ligands, one coordinated EtOH molecule, one coordinated dmf molecule, and one uncoordinated dmf molecule. The $\mathbf{L}^4$ ligand adopts a syn conformation with an average dihedral angle between the central benzene ring and the side benzene ring of 108.9°, which is slightly smaller than that of $\mathbf{L}^3$ in complex **3**. Different solvent molecules occupy the axial positions of the paddlewheel. As shown in Figure 5e,h, two coordinated EtOH molecules locate outside of the cage, while two coordinated dmf molecules locate inside, which prevents other solvent molecules from entering. The different axially coordinated solvates on the paddlewheel SBU reduce the symmetry of **4** and make it a distorted cage from an ideal $I4$ symmetry. The distance between the copper ions in different paddlewheel SBUs is 9.175 Å, and the volume of the cage is about 638 $Å^3$, which is slightly larger than that of complex **3**.

Single-crystal X-ray diffraction reveals that complex **5** is a MOCC based on a binuclear manganese SBU. Different from complexes **3** and **4**, the binuclear manganese SBU in **5** is formed by two carboxylate groups and one bridging water molecule. The MOCC of **5** consists of two binuclear manganese SBUs and four $\mathbf{L}^4$ ligands, as shown in Figures 5c,f,i. The crystal structure of **5** was described in a previous communication.[12] Complex **5** was synthesized in a conventional condition in mixed solvents of DMF/EtOH/H_2O. However, when a similar reaction was run in DMF, light-brown block crystals of **6** were obtained in good yield. Single-crystal X-ray diffraction reveals that complex **6** crystallizes in a monoclinic $P2_1/n$ space group and possesses a 1D coordination polymer based on a trinuclear hourglass SBU. The asymmetric unit consists of three manganese ions, three $\mathbf{L}^4$ ligands, four coordinated dmf molecules, and three water and one dmf guest molecules. The three manganese ions are engaged by six carboxylate groups from different $\mathbf{L}^4$ ligands to generate the "hourglass" SBU (Figure 6a), which is similar to that found in complex **2**. The average Mn−O distance is 2.192 Å, which is slightly longer than that in **5**. Both carboxylate groups of the $\mathbf{L}^4$ ligand are deprotonated during the reaction. Similar to **5**, the two carboxylate groups of the $\mathbf{L}^4$ ligand possess different coordination modes: one adopts a bidentate bridging mode to connect two manganese ions and the other one adopts a chelate bridging mode to link two manganese ions. The average dihedral angle between the central benzene ring and the side benzene ring is 96.2°, which is larger than that in **5**.

Thus, the trinuclear manganese "hourglass" SBU is infinitely connected by the bent $\mathbf{L}^4$ ligand to generate a 1D coordination polymer containing cages (Figure 6d). Different from **5**, the cage consists of three $\mathbf{L}^4$ ligands and two manganese ions (Figure 6b,c). Three coordinated dmf molecules are inside the cage. The Mn−Mn distance in different vertexes of the cage is 7.667 Å, which is slightly longer than that in **5**. If the Mn1 or Mn3 ions can be

considered as the vertexes and the L^4 ligands as the edges of the cage, then the 1D chain is formed by an infinite connection of the cages sharing the Mn2 ions, as shown in Figure 6e.

Thermal Stabilities for 1−6. TGA was carried out to examine the thermal stabilities of complexes **1**−**6** (Figure S8 in the Supporting Information). Samples were heated under a nitrogen atmosphere to 600 °C. For complex **1**, the first weight loss of 3.1% from 55 to 110 °C is in accordance with the loss of one uncoordinated and two coordinated water molecules (calcd: 3.6%), and the second weight loss of 9.3% from 110 to 162 °C corresponds to the loss of two coordinated dmf molecules (calcd: 9.7%). The third weight loss of 9.9% from 162 to 256 °C corresponds to the loss of the two remaining coordinated dmf molecules (calcd: 9.7%), and after a stable stage in the range 260−320 °C without any weight loss, the metallamacrocycle starts to decompose beyond 320 °C. For complex **2**, there are two steps of weight loss from 50 to 285 °C: the first weight loss of 15.9% from 50 to 160 °C is in accordance with the loss of two coordinated water molecules and four uncoordinated dmf molecules (calcd: 16.2%), and the second weight loss of 9.5% from 160 to 285 °C corresponds to the loss of two coordinated dmf molecules and one uncoordinated dmf molecule (calcd: 10.8%). There is no weight loss from 285 to 320 °C, and after that, **2** starts to decompose. For complex **3**, the gradual weight loss of 8.6% from 50 to 245 °C is in accordance with the loss of three uncoordinated dmf molecules (calcd: 9.3%). The loss of the coordinated water molecules in **3** is not observed before 245 °C, where decomposition starts. For complex **4**, there is no weight loss from 50 to 150 °C, and the gradual weight loss of 25% from 150 to 295 °C corresponds to the loss of eight uncoordinated DMF molecules, six uncoordinated water molecules, and two coordinated EtOH molecules (calcd: 26.3%). The loss of the coordinated dmf molecule inside the cage in **4** is not observed before 295 °C, where decomposition starts. Complex **5** can be stable up to 320 °C. The first weight loss of 15.5% from 50 to 140 °C corresponds to the loss of one uncoordinated water and six uncoordinated dmf molecules (calcd: 16%). The second weight loss of 13% from 140 to 300 °C corresponds to the loss of four coordinated dmf and four coordinated water molecules (calcd: 12.8%), and after 320 °C, **5** starts to decompose. For complex **6**, the first weight loss of 16% from 50 to 150 °C corresponds to the loss of three uncoordinated water molecules, two uncoordinated dmf molecules, and two coordinated dmf molecules (calcd: 17.2%), and the second weight loss of 7.9% from 150 to 270 °C corresponds to the loss of two coordinated dmf molecules (calcd: 7.3%); there is no weight loss from 270 to 330 °C, and after 330 °C, **6** starts to decompose.

Magnetic Properties of Complexes 5 and 6. The magnetic properties of complexes **5** and **6** were investigated over the temperature range 2−300 K. The results are displayed in the form of χT vs T plots, with T being the absolute temperature (Figure 7). For complex **5**, the χ_M value is 0.0516 $cm^3\ mol^{-1}$ at 300 K. As the temperature is lowered, the χ_M value increases gradually and reaches a maximum of 0.3996 $cm^3\ mol^{-1}$ at 9 K and then decreases

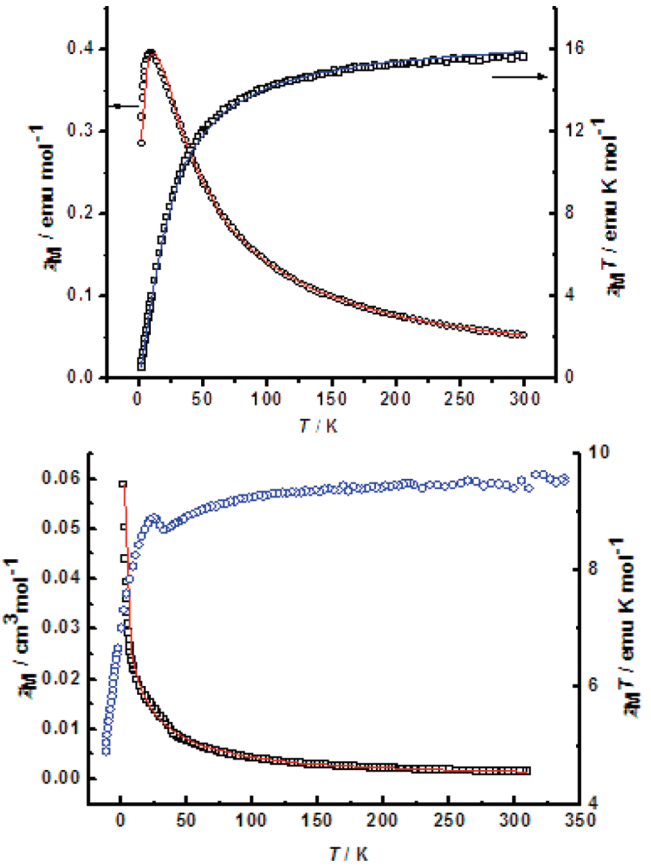

Figure 7. Experimental χ_M vs T and $\chi_M T$ vs T curves for **5** (top) and **6** (bottom).

to 0.2868 $cm^3\ mol^{-1}$ at 2 K, which indicates weak antiferromagnetic coupling between the manganese centers.[15] The $\chi_M T$ value is 15.65 $cm^3\ mol^{-1}$ K at 300 K, which decreases gradually as the temperature is decreased, reaching 0.29 $cm^3\ mol^{-1}$ K at 2 K. To determine the magnitude of the exchange interaction, the χ vs T data were fitted by least squares using the following equation:

$$\chi_{di} = [Ng^2\beta^2 S(S+1)/kT](A/B)$$

$$A = 110\exp(12.5J/kT) + 60\exp(2.5J/kT) + 28\exp(-5.5J/kT) + 10\exp(-11.5J/kT) + 2\exp(-15.5J/kT)$$

$$B = 11\exp(12.5J/kT) + 9\exp(2.5J/kT) + 7\exp(-5.5J/kT) + 5\exp(-11.5J/kT) + 3\exp(-15.5J/kT) + \exp(-17.5J/kT)$$

where χ_{di} refers to the molar susceptibilities of **5**. The intramolecular exchange constant J is defined for the isotropic Heisenberg−Dirac−van Vleck (HDVV) exchange Hamiltonian ($H = 2JS_1S_2$, with $S_1 = S_2 = {}^5/_2$) for binuclear complexes. The parameters were optimized to fit χ_{di} as a function of the temperature. An excellent fit was obtained with $J = -1.307 \pm 0.005$ cm^{-1} and $g = 1.966 \pm 0.003$ with an agreement factor R of 8.37×10^{-5}. This result also indicates weak antiferromagnetic coupling between

(15) Mukherjee, P. S.; Konar, S.; Zangrando, E.; Mallah, T.; Ribas, J.; Chaudhuri, N. R. *Inorg. Chem.* **2003**, *42*, 2695.

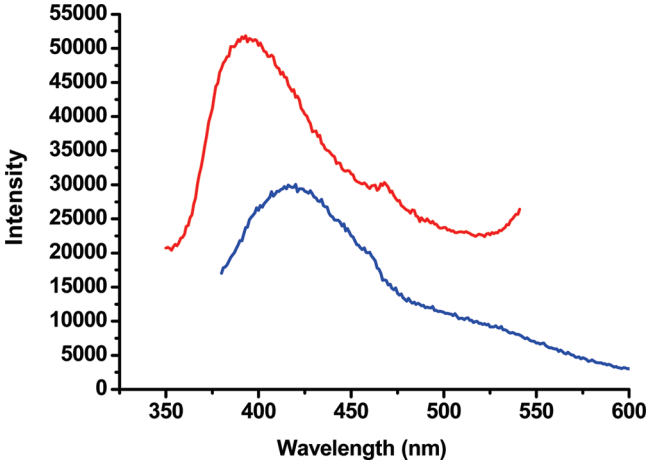

Figure 8. Solid-state emission spectra of free H_2L^1 (red) and **1** (blue).

two manganese centers through the carboxylate and coordinated water bridges. On the basis of the discrete cage connectivity, two effective magnetic exchange pathways are present within the cage through carboxylate bridges and a bridging water molecule,[16] with the shortest Mn····Mn distance being 3.54 Å.

For complex **6**, the χ_M value is 0.001 57 $cm^3\ mol^{-1}$ at 300 K. As the temperature is lowered, the χ_M value increases gradually and reaches 0.059 $cm^3\ mol^{-1}$ at 2 K, which indicates weak antiferromagnetic coupling between the manganese centers. The $\chi_M T$ value is 9.55 $cm^3\ mol^{-1}$ K at 300 K, which decreases gradually as the temperature is decreased, reaching 4.90 $cm^3\ mol^{-1}$ K at 2 K. To determine the magnitude of the exchange interaction, the χ vs T data were fitted by least squares using the following equation:

$$\chi_M^J = 3Ng^2\beta^2/kT(A/B)$$
$$A = 55 + 30\exp(-10J/kT) + 14\exp(-18J/kT) + 5\exp(-24J/kT) + \exp(-28J/kT)$$
$$B = 11 + 9\exp(-10J/kT) + 7\exp(-18J/kT) + 5\exp(-24J/kT) + 3\exp(-28J/kT) + \exp(-30J/kT)$$
$$\chi_M^{J+J'} = \chi_M^J/(1 - zJ'\chi_M^J/Ng^2\beta^2)$$

The intramolecular exchange constant J is defined for the isotropic HDVV exchange Hamiltonian [$H = -2J(S_1S_2 + S_2S_3 + S_3S_1) = -6JS_1S_2$, with $S_1 = S_2 = S_3 = {}^5/_2$] for trinuclear complexes. The parameters were optimized to fit χ_M as a function of the temperature. An excellent fit was obtained with $J = -0.19\ cm^{-1}$, $J' = -0.26\ cm^{-1}$, and $g = 2.45$ with an agreement factor R of 6.9×10^{-8}. This result indicates weak antiferromagnetic coupling between three manganese centers through the carboxylate bridges, with the shortest Mn···Mn distance being 3.481 Å.

Photoluminescence Properties for 1. Photoluminescence measurements of **1** in the solid state at room temperature show that complex **1** exhibits strong luminescence at $\lambda_{max} = 420$ nm, upon excitation at 360 nm (Figure 8). This emission can be assigned to a metal-to-ligand charge transfer because free H_2L^1 possesses strong emission at $\lambda_{max} = 390$ nm in the solid state, a 30 nm shift observed compared to complex **1**.

(16) Wang, J.; Lin, Z.-J.; Ou, Y.-C.; Shen, Y.; Herchel, R.; Tong, M.-L. *Chem.—Eur. J.* **2008**, *14*, 7218.

Scheme 3. Schematic Representation of a Metallamacrocycle, a MOCC, and Their Extensions to 1D or 2D Coordination Polymers

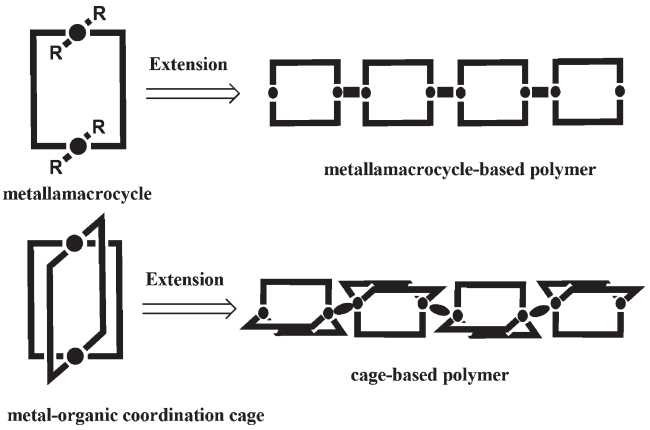

Conclusions

Six novel metal−organic supramolecules based on flexible dicarboxylate ligands have been designed and synthesized. The results and conclusions of these investigations are summarized as follows: (1) The ligand geometry or conformation plays an important role in the formation of discrete supramolecules. In particular, the syn conformation of the flexible ligands is apt to form a metallamacrocycle or MOCC based on the difference of the metal ion or cluster. (2) Using manganese or copper ions to assemble with flexible ligands is helpful for the formation of MOCC because the manganese and copper ions, compared to the cadmium ion, are apt to form 4-connected binuclear metal clusters. (3) Some metal−organic supramolecules (**1** and **5**) possess discrete structural units, such as metallamacrocycles, MOCCs, etc. These discrete metal−organic supramolecules can act as intermediate building units to further extend into 1D or 2D coordination polymers (**2** and **6**), as shown in Scheme 3.

Herein we have demonstrated the use of flexible dicarboxylate ligands with the appropriate angles to create functionalized metal−organic supramolecules. In a continuation of these studies, we may gain a more in-depth understanding of discrete molecule assembly using flexible dicarboxylate ligands and may design new functionalized metal−organic supramolecules such as metallamacrocycles and MOCCs for a wide range of potential applications.

Acknowledgment. We are grateful for financial support from the NSF of China (Grants 90922014 and 20701025), the NSF of Shandong Province (Grant Y2008B01), and Shandong University.

Supporting Information Available: Six X-ray crystallographic files in CIF format and structural figures and TGA for complexes **1**−**6**. This material is available free of charge via the Internet at http://pubs.acs.org.